Biosensors and Bioelectronics 172 (2021) 112779

Contents lists available at ScienceDirect

Biosensors and Bioelectronics

journal homepage: http://www.elsevier.com/locate/bios

The investigation of detection and sensing mechanism of spicy substance based on human TRPV1 channel protein-cell membrane biosensor

Sa Xiao [a,1], Panpan Song [a,1], Fanjie Bu [a], Guangchang Pang [a], Aimin Zhou [b], Yanqing Zhang [a,*], Junbo Xie [c,**]

[a] Biotechnology & Food Science College, Tianjin University of Commerce, Tianjin, 300134, China
[b] Department of Chemistry, Center for Gene Regulation in Health and Diseases, Cleveland State University, Cleveland, OH, 44115, USA
[c] School of Chinese Materia Medica, Tianjin University of Traditional Chinese Medicine, Tianjin, 301617, China

ARTICLE INFO

Keywords:
Human TRPV1 channel protein
Cell membrane biosensor
Capsaicin
Activation constant
Molecular docking

ABSTRACT

The transient receptor potential vanilloid 1 (TRPV1) is a key target for the spicy taste sensor and analgesic drug development. However, the human TRPV1-associated signaling remains to be obscure. In this study, we over-expressed human TRPV1 (hTRPV1) in HEK293T cells and explored its signaling activated by spicy substances. A cell membrane biosensor was constructed by using the cells highly expressed hTRPV1 through a layer-by-layer assembly. Our results showed that the activation constants by capsaicin, allicin and sanshool, the active components of chili pepper, garlic and mountain pepper, were $K_{a,\ capsaicin} = 3.5206 \times 10^{-16}$ mol/L, $K_{a,\ allicin} = 5.0227 \times 10^{-15}$ mol/L, $K_{a,\ sanshool} = 1.7832 \times 10^{-15}$ mol/L. Obviously, the order of the sensitivity mediated by hTRPV1 was capsaicin > sanshool > allicin. The affinity values of the three spicy substances with hTRPV1 analyzed by molecular docking simulation also displayed the same law. Most importantly, some amide bonds and their similar groups and even benzene rings of spicy compounds were fund to be critical in the spicy sensing process. In addition, Glu570 in the active pocket of hTRPV1 plays an important role in identifying spicy substances. The elucidation of the detailed mechanism mediated by hTRPV1 in spicy sensing will lay a theoretical foundation to design rational strategies for screening of potential analgesics.

1. Introduction

The research of receptor-type ion channels has always been the focus of attention, not only because it can play a role in identifying the specific ligands, but also the channels can change the intracellular ion level to affect the life activities of the cell. Transient receptor potential (TRP) channels belong to the superfamily of sensory-related ion channels, which respond to a variety of thermal, mechanical, or chemical stimuli (Nilius and Szallasi, 2014). The transient receptor potential vanilloid 1 (TRPV1) is a well-studied member of the TRP family, involving a series of functions such as spicy taste, pain and inflammation (Cui et al., 2016). As a non-selective cation channel, it can be activated by harmful temperature higher than 43 °C, spicy substances (capsaicin, allicin, etc.), lipids, tissue injury stimulators and arachidonic acid metabolites and other endogenous factors, thus leading to the occurrence and development of pungency sensing, pain transduction and inflammatory responses (Liu et al., 2009). Therefore, Understanding the TRPV1 ligands-mediated mechanism of sensing is of great significance in food, drug, and physiological and pathological research.

Currently, the main methods for determining spicy substances are Scoville Heat Units (SHU) sensory evaluation and high performance liquid chromatography (HPLC) (Govindarajan et al., 1977; Weaver et al., 1984; Gonzalez-Zamora et al., 2013). The advantage of the SHU sensory evaluation method is that it can provide the sensory characteristics of spicy substances, which is more similar to the actual feeling of human body. However, the objectivity and accuracy of the assessment are limited by the differences in individual sensitivity and tolerance of sensory assessors (Njoman et al., 2017). HPLC can detect the true components of spicy substances in food, but the degree in activating the sensing of taste bud cells through TRPV1 by different spicy substances may be quite different (Watanabe and Terada, 2015). The difference in the Ca^{2+} influx and action potentials of taste bud cells upon stimulation

* Corresponding author. Biotechnology & Food Science College, Tianjin University of Commerce, Tianjin, 300134, China.
** Corresponding author.
E-mail addresses: zhyqing@tjcu.edu.cn (Y. Zhang), xiejb@tjutcm.edu.cn (J. Xie).
[1] These authors contributed equally to this work.

https://doi.org/10.1016/j.bios.2020.112779
Received 26 September 2020; Received in revised form 26 October 2020; Accepted 28 October 2020
Available online 1 November 2020

ultimately results in distinctive spicy sensation (Qiao et al., 2015). This outcome is probably due to the unique molecular structure of various spicy substances, which displays different affinity with the TRPV1 active pocket. Therefore, the types and components of spicy substances cannot truly present the real spicy feeling of human beings. In recent years, an electronic tongue has been developed as a new generation of the tasting technology, which can be used for detecting a variety of tastes including sour, salty, sweet, umami, and bitter (Tahara and Toko, 2013). Courtney and Victoria used electronic tongues to detect spicy compounds (Schlossareck and Ross, 2019; Paup et al., 2019), which is based on the difference in the potential changes of the artificial lipid membrane caused by different spicy substances. Different from the recognition and sensing of the capsaicin receptor (TRPV1), whether this potential change can represent the true spicy taste remains to be further investigated. Therefore, it is urgent to develop novel analytical methods to more accurately, objectively and truly evaluate the sensing for spicy substances.

Recent years, biosensors developed by fixing biological sensitive elements on the different supporting materials have made tremendous progress in studying enzyme functions, ligand and receptor interaction, cell signaling and other aspects. In our preliminary work, Qiao et al. prepared biosensors by immobilizing SD rat taste bud tissues to detect capsaicin and gingerol (Qiao et al., 2015). After that, we successfully screened several TRPV1 antagonists using the taste bud tissue sensor, and analyzed the relationship between structure and function (Xiao et al., 2019). The information provides a new direction for the development of analgesic drugs. Although the SD rat taste bud tissue sensor can be successfully used for the detection of spicy substances and screening of TRPV1 antagonists, it is inevitable to directly study human TRPV1 channel proteins (hTRPV1) under the premise that all studies are aimed at serving human beings. This is because the results obtained with animal TRPV1 as the research object add uncertain factors to the analysis of actual human conditions. However, the difficulty in obtaining human tissues and ethical issues severely limit the direct research of hTRPV1. Therefore, only hTRPV1 receptors or cells and other materials can be used for research. In the field of biosensors, the construction of cell sensors is difficult due to problems such as cell activity and stability, and the development of single-molecule sensors with immobilized enzymes or receptors is the most in-depth. Therefore, direct immobilization of free hTRPV1 seems to be a good choice. However, hTRPV1 is a membrane channel protein with dual functions of receptor and ion channel. In recent years, several research have revealed the activation mechanism of vanilloid ligands on TRPV1 channels (Hammond et al., 2012; Cao et al., 2013; Gao et al., 2016). This activation mechanism conveys an important message that the switching process of the TRPV1 channel on/off state needs to maintain the conformation of the TRPV1 transmembrane domain. The integrality of six transmembrane structure is essential for TRPV1 channel to execute its function. Some researchers have achieved the immobilization of other ion channels in vitro by using artificial lipid membranes and obtained anticipated results (UTO et al., 1990; Cornell et al., 1997; Oh et al., 2008). Different from the use of artificial lipid membranes, in this study, we hope to use the most primitive cell membrane structure as a carrier to achieve the immobilization of TRPV1 channel closer to the physiological state.

Therefore, in this study, we overexpressed hTRPV1 in HEK293T cells by using genetic engineering technology, and constructed a novel cell membrane (CM) biosensor by directly immobilizing the cell membrane of HEK293T cells with hTRPV1 based on the characteristics of cytoskeleton proteins and extracellular matrix proteins. The biosensor was successfully used to detect capsaicin, allicin and sanshool. More importantly, it was able to distinguish the activation intensity of hTRPV1 by different spicy substances. Furthermore, the molecular mechanism by which hTRPV1 interacts with the three spicy substances was determined at its amino acid level via molecular docking.

2. Materials and methods

2.1. Materials, equipment and pretreatment of glassy carbon electrode

The list of reagents, materials and equipment used in this work and pretreatment of glassy carbon electrode are provided in the Supplementary material.

2.2. Establishment of HEK293T cell line stably expressing hTRPV1

Firstly, pcDNA3.1 (+) eukaryotic expression vector containing the gene of hTRPV1 (NCBI reference sequence: NM_080705.4) was constructed (Caterina et al., 1997), and the plasmid vector was transformed into the competent *Escherichia coli* cells to obtain the engineered strain. Subsequently, the engineering bacteria were amplified using selective Luria-Bertani medium containing 100 μg/mL ampicillin, and a large number of high-purity target plasmids were obtained by endotoxin-free plasmid extraction. Then pcDNA3.1 (+) was transfected into HEK293T cells by lipofection. After transfection, the cells were screened in the medium containing G418. Finally, agarose gel electrophoresis and Western blot experiments were used to verify the successful construction of pcDNA3.1 (+) vector containing hTRPV1 gene sequence and the expression of hTRPV1 on the cell membrane of stably transfected HEK293T cells. Specific steps for establishing a HEK293T cell line stably expressing hTRPV1 are provided in Supplementary materials.

2.3. Construction of hTRPV1-cell membrane biosensor

2.3.1. Preparation of cell membrane suspension

The preparation method of the cell membrane is as follows. The cultured hTRPV1-HEK293T cells were transferred to a 15 mL centrifuge tube and centrifuged at 800 rpm (86×*g*) for 3 min to obtain the cell precipitation. Then 10 mL Tris-HCl buffer solution (pH = 7.4) was added into the centrifuge tube to resuspend and disperse the cells, and then 300 μL 100 mmol/L phenylmethylsulfonyl fluoride (PMSF) was added to fully mix. The cells were disrupted by ultrasonic in an ice bath. The ultrasonic parameters were set as follows: 3s ultrasonic time, 3s interval time, 20 times, 150 W power. The broken cell debris suspension was centrifuged at 1000 rpm (134×*g*) for 10 min at 4 °C, and the supernatant was centrifuged at 15000 rpm (29988×*g*) for 20 min to obtain a cell membrane precipitation. Finally, an appropriate amount of Tris-HCl (pH = 7.4) was used to remix the cell membrane precipitation to obtain a cell membrane suspension.

2.3.2. Preparation of nano-gold and reduced graphene oxide (RGO)

The nano-gold solution was prepared by thermal reduction method (Boisselier and Astruc, 2009). First, transfer 100 mL of 0.01 g/100 mL of chloroauric acid solution and 4 mL of 1 g/100 mL of sodium citrate solution to a clean Erlenmeyer flask, and then heat the mixture in a microwave oven at low heat until the solution appears translucent wine red. The prepared nano-gold solution should be stored in the dark at 4 °C.

The preparation of RGO refers to Lei's work with some melioration (Lei et al., 2017). 30 mg of monolayer graphene oxide (GO) was dispersed in 30 mL of water by ultrasonic treatment. The pH of the GO suspension was adjusted to 9–10 using a 5% sodium carbonate solution, and then 240 mg of sodium borohydride was added. Then the mixture was stirred at 750 rpm for 1 h at 80–90 °C. During the reduction process, the GO dispersion changed from dark brown to black. The RGO precipitate was obtained by centrifugation at 5000 rpm (3354×*g*) for 10 min, and the resulting precipitate powder was freeze-dried overnight. The dried powder was resuspended with 0.5% chitosan solution by ultrasound to obtain 1 mg/mL RGO solution, which was sealed and stored for future use.

2.3.3. Assembly of hTRPV1-cell membrane biosensor

The GCE is first pretreated using the method described in the Supplementary material. Then, the ultrasonically dispersed 1 mg/mL RGO chitosan solution was dripped on the surface of the pretreatment electrode, dried naturally at room temperature, and rinsed off the unbound RGO with ultrapure water. A fresh thionine-chitosan (Thi-Chit) solution was prepared by mixing 2% chitosan and 0.01 mol/L thionine in 2% acetic acid solution. Thi-Chit solution was applied dropwise to the surface of RGO modified electrode to obtain Thi-Chit/RGO/GCE. Then put the above electrode into the pre-prepared nano-gold solution and self-assemble at 4 °C for 24 h. After washing off the unbound nano-gold, the electrode was immersed in 18 mmol/L cysteamine (CA) aqueous solution for 4 h at room temperature in the dark (Xia et al., 2017). The electrode was then taken out of the CA solution and rinsed with ultrapure water to remove physically adsorbed CA. Finally, it was dried with N_2 to form CA/AuNP/Thi-Chit/RGO/GCE. The electrode was then incubated with 100 μg/mL intermediate filaments (IF) for 2 h by EDC/NHS catalysis to fix the intermediate filaments on the electrode (Viswanathan et al., 2012). Then the electrode was immersed in the prepared cell membrane suspension to self-assemble for 12 h at 4 °C. Through the specific binding of intermediate filaments to the cell membrane, the cell membrane is controllably fixed on the electrode surface. Finally, 100 μg/mL type I collagen (CoI) was used to encapsulate the cell membrane to maintain cell membrane adhesion and viability (Jiang et al., 2013). Finally, CoI/CM/IF/CA/AuNP/Thi-Chit/RGO/GCE biosensors were successfully prepared. The electrode preparation process is shown in Fig. 1A. Fig. 1B shows the detection principle of the biosensor. hTRPV1 is used as the biological recognition element of the electrode, which can specifically bind to spicy substances. On the one hand, spicy substances are adsorbed to the hTRPV1 on the electrode surface, on the other hand, the activated hTRPV1 will also undergo conformational changes. These factors together lead to the change of electrode surface resistance, thereby affecting the current. During the preparation of hTRPV1-cell membrane biosensors, each step was characterized by cyclic voltammetry (CV) and electrochemical impedance spectroscopy (EIS) in 1×10^{-3} mol/L $K_3Fe(CN)_6$ solution (containing 0.2 mol/L KNO_3).

2.4. Detection of spicy substances

Three-electrode system was used for measurement: hTRPV1-cell membrane GCE as working electrode, Ag/AgCl electrode (saturated KCl) as reference electrode and platinum wire electrode as counter electrode. Ultrapure water is used as the test base fluid. The response current of the prepared hTRPV1-cell membrane biosensors to capsaicin, allicin and sanshool was measured by amperometric i-t curve method. The response current change rate is used as a detection index and the calculation formula is shown in Eq. (1).

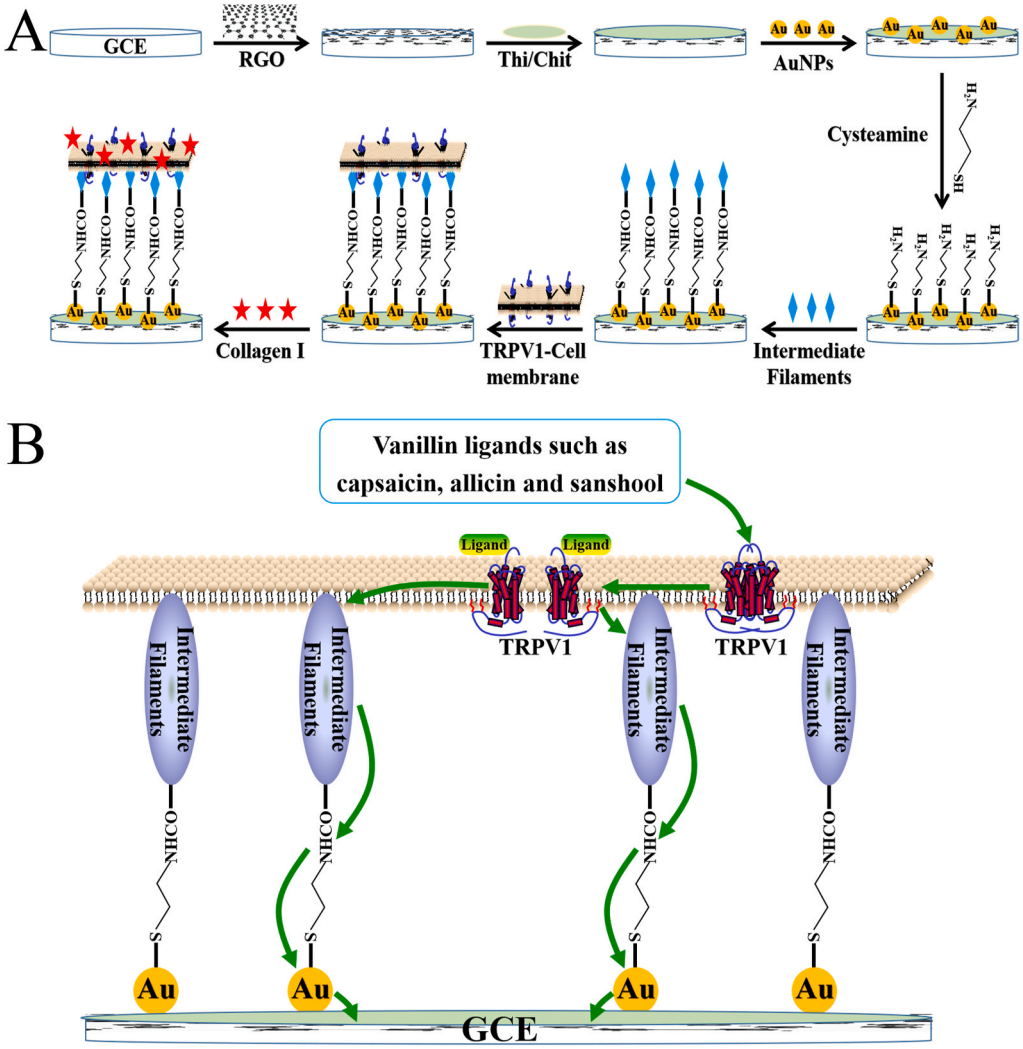

Fig. 1. Preparation process (A) and detection schematic diagram (B) of hTRPV1-cell membrane biosensor.

$$\Delta I \Big/ \% = \frac{I_1 - I_2}{I_1} \times 100 \quad (1)$$

Among them, I_1 and I_2 refer to the steady state current values at the same time point before and after the determination, respectively.

2.5. Molecular docking

2.5.1. Homology-modelling of the 3D structure of hTRPV1

In order to verify the results of the hTRPV1-cell membrane biosensor for detecting spicy substances, we used molecular docking to study the binding modes of three spicy substances and hTRPV1. Molecular docking is a theoretical simulation method to predict the binding mode and affinity of ligand and receptor based on the geometric structure, energy and chemical environment of the ligand molecule and receptor protein. The molecular docking process is based on the three-dimensional (3D) structure of the ligand and the receptor, and the optimal energy conformation of the ligand-receptor complex is screened through a calculation function. Unfortunately, at present, the 3D structure of hTRPV1 has not been determined. Therefore, the amino acid sequence of the expressed hTRPV1 was searched by BLAST in the protein database (PDB). It was found that the hTRPV1 has a high degree of homology (>80%) with the TRPV1 of rattus norvegicus. Therefore, we carried out homology-modelling of the 3D structure of hTRPV1 through the SWISS-MODEL server (Waterhouse et al., 2018; Guex et al., 2009; Bienert et al., 2017; Studer et al., 2020; Bertoni et al., 2017).

2.5.2. hTRPV1 processing and ligand preparation

The hTRPV1 protein and ligand need to be treated before molecular docking. First, by using AutoDockTools, the water molecules and ions of the hTRPV1 A chains ($hTRPV1_A$) were deleted, and then polar hydrogen atoms were given to $hTRPV1_A$ (Sanner, 1999; Morris et al., 2009). Then, we obtained the two-dimensional (2D) molecular structure of capsaicin, allicin and sanshool by ChemDraw. Then, the energy optimization of the 3D structures of the three spicy substances was carried out in Chem3D using the MM2 method, and the lowest energy conformation was selected as the initial conformation before molecular docking.

2.5.3. Molecular docking parameter setting

Using resiniferatoxin (6EU) as the reference ligand, AutoDockTools were used to determine the parameters of the active pocket of $hTRPV1_A$ (Sanner, 1999; Morris et al., 2009). First, the Gridbox center coordinates were set to center_x = 114.24, center_y = 139.226, and center_z = 129.406. Second, the 3D structure of the ligand needs to be fully contained in the Gridbox. Therefore, the Gridbox size was set to size_x = 15, size_y = 15, size_z = 15. Other parameters are default values.

2.5.4. Feasibility verification of molecular docking

It is necessary to check the reliability of the docking procedure and the set parameters before docking. First, we extracted 6EU from the structure of $hTRPV1_A$-6EU, and then the 6EU was re-docked back into the active pocket of $hTRPV1_A$ by using AutoDock Vina software (Trott and Olson, 2010). Finally, PyMol software is used to obtain the visualization results (The PyMOL Molecular Graphics System, Version 2.4 Schrödinger, LLC.).

2.5.5. Molecular docking of spicy substances with $hTRPV1_A$

After confirming the feasibility of the docking method, this study uses semi-flexible docking method to study the mechanisms of capsaicin, allicin and sanshool to activate $hTRPV1_A$ respectively through AutoDock Vina software (Trott and Olson, 2010). The docking parameter settings are as described above. According to the Lamarckian Genetic Algorithm (LGA), the AutoDock Vina program continuously adjusts the conformation of the ligand molecule with a flexible structure within the Gridbox range, and then scores the different conformations of the ligands (including orientation, position and energy) (Morris et al., 1998). During the docking process, each spicy substance produced 9 docking conformations, and each conformation was ranked according to the affinity value from high to low. The result of the highest affinity value is that the conformation of ligand molecule and receptor protein reaches the best geometric and energy matching. Subsequently, PyMol and BIOVIA Discovery Studio software were used to analyze the binding mode and interaction of the three spicy substances with $hTRPV1_A$.

2.6. Data analysis

The sensor data were analyzed and processed using Origin 8.0 software (OriginLab Northampton, MA) and GraphPad Prism 8 (GraphPad Software, USA). The limit of detection (LOD) was defined as the target concentration giving a response current signal at least three times different from the standard deviation of the blank control signal.

3. Results

3.1. Overexpression of hTRPV1 in HEK293T cell line

The pcDNA3.1 (+) expression vector after restriction enzyme *Eco*RI/*BamHI* digestion was verified by agarose gel electrophoresis. As shown in Fig. S1, agar-gel electrophoresis results showed two distinct bands, among which the band between 2500 bp and 3000 bp was consistent with the sequence length of hTRPV1 gene (2538 bp), while the band between 5000 bp and 6000 bp was pcDNA3.1 (+) plasmid vector (5.4 kb). In addition, DNA sequencing results showed that nucleotide sequence of hTRPV1 gene in plasmid pcDNA3.1 (+) was the same as reported in the reference (Caterina et al., 1997). The results showed that the plasmid vector containing hTRPV1 gene was constructed successfully.

Mem-PER™ Plus Membrane Protein Extraction Kit was used to extract the membrane proteins of HEK293T cells stably transfected and not transfected. Then the expressing level of hTRPV1 in the clonal cells was determined by Western blot analysis. The results are shown in Fig. S2. The membrane protein of transfected HEK293T cells displays a clear band at 95 kD, which proves that hTRPV1 is not only stably expressed in transfected HEK293T cells, but also can locate the cell membrane to function as a capsaicin receptor. In addition, the untransfected HEK293T cells has no visible band at 95 kD. This indicates that the hTRPV1 on the cell membrane of HEK293T cells is synthesized and expressed by the pcDNA3.1 (+) plasmid, rather than the HEK293T cells themselves. And hTRPV1 can automatically locate on the cell membrane.

3.2. Characterization of nano-gold and RGO

The prepared nano-gold was characterized by ultraviolet spectroscopy (UV) and transmission electron microscope (TEM). Studies have shown that the maximum UV absorption wavelength of nano-gold gradually red shifts as the particle size of nano-gold increases (Link and El-Sayed, 1999). As shown in Fig. S3A, the maximum UV absorption wavelength of the prepared nano-gold is 521 nm, indicating that the particle size of the nano-gold is about 22 nm. More precisely, the TEM results of nano-gold in Fig. S3B showed that the prepared nano-gold was round with the particle size about 15 nm. Furthermore, the nano-gold particles were evenly dispersed without obvious aggregation. Apparently, the TEM and UV analysis results were consistent, suggesting that the prepared nano-gold was suitable for modifying GCE.

The GCE modified by GO or RGO was characterized by using a CV method. Interestingly, the oxidation-reduction peak current was significantly increased while the graphene was being assembled on the surface of the pretreated GCE as shown in Fig. S4. The phenomena may be due to the capability of graphene in super-conductivity, high carrier mobility and extremely low electronic noise because of its spatial quantum tunneling structure (Chang et al., 2014). In addition, graphene also has a

specific surface area with high nanoparticle adsorption characteristics, which allows it to combine with metal nanoparticles or other carbonaceous materials (such as carbon nanotubes) into a polymer to produce novel nanomaterials with enhanced optical and electrical properties (Palmieri et al., 2016; Chavez-Valdez et al., 2013). In addition, the peak current value increased by RGO was significantly higher than that of GO. This may be due to the large number of oxygen-containing groups on the GO surface, including hydroxyl groups, epoxy functional groups, carbonyl groups, carboxyl groups and so on, which reduce the electron transport ability of the electrode modified interface (Zhu et al., 2010). A appropriate reduction method reduces the number of oxygen-containing groups on the GO surface, which restores the relatively complete planar conjugated structure of graphene and improves its conductivity. Therefore, the RGO-modified GCE has a larger response current under the same voltage conditions.

3.3. Electrochemical characterization of the hTRPV1-cell membrane biosensor

Each step in the assembly process of hTRPV1-cell membrane biosensor was characterized by CV and EIS. The result is shown in Fig. 2. First of all, the redox peak current of RGO modified pre-treated GCE is significantly increased. And the approximate linear EIS also shows that the electrode surface impedance is significantly reduced. This not only indicates that RGO has been modified to the electrode surface, but also significantly improves the electron mobility and conductivity of the electrode surface. When Thi-Chit was modified on the electrode surface,

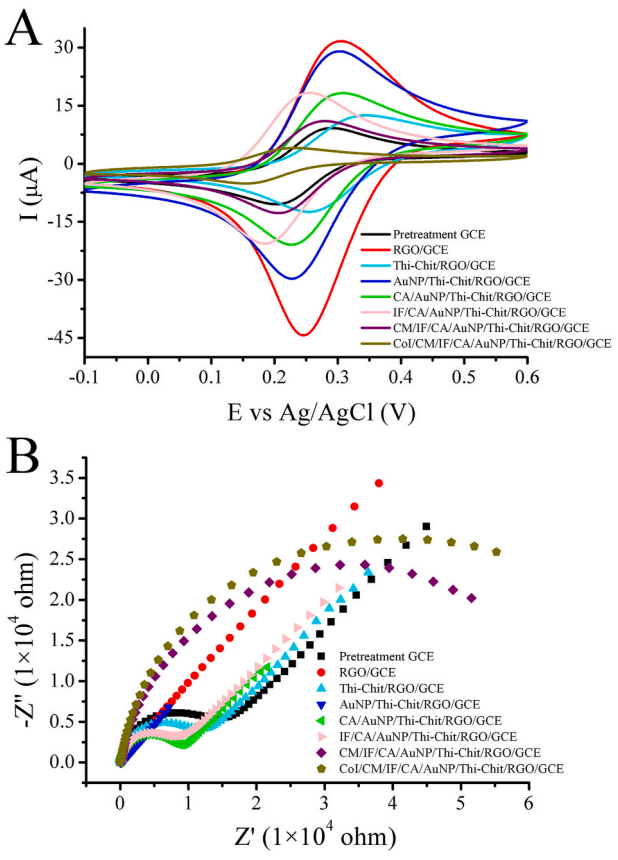

Fig. 2. Electrochemical characterization of hTRPV1-cell membrane biosensor assembly process. (**A**) Cyclic voltammogram obtained at a scan rate of 50 mV/s over a voltage range of −0.1–0.6 V. (**B**) The electrochemical impedance spectroscopy is scanned under the condition that the initial voltage is the open circuit potential and the frequency range is 10^{-2} Hz–10^{6} Hz. The characterization solution is 1×10^{-3} mol/L $K_3Fe(CN)_6$ solution (containing 0.2 mol/L KNO_3).

the redox peak current was significantly reduced and the impedance increased compared with RGO modification. This is because although thionine (as an electron mediator) can enhance the movement of electrons, chitosan is a material that can hinder electron migration (Gerbino et al., 2008; Wu et al., 2020). The reason why chitosan is used to modify electrode is that chitosan has excellent biocompatibility, which can provide a good carrier for biological detection elements (Kumar et al., 2004). Subsequently, a layer of nano-gold was loaded on the surface of Thi-Chit to improve the peak current. Due to the excellent electrical conductivity and the increased effective area of the electrode, the nano-gold modification significantly increased the current and reduced the impedance. Then the formation of Au–S bonds connects cysteamine to the electrode surface, so that the exposed amino group of cysteamine can be combined with the intermediate filaments in the form of an amide bond through EDC/NHS catalysis. The modification of cysteamine and intermediate filaments led to the decrease of $Fe(CN)_6^{3-/4-}$ peak current and the increase of electrode surface impedance. This phenomenon is attributed to the fact that cysteamine molecules and intermediate filaments hinder the reaction of the redox probe. As a cytoskeleton protein, intermediate filaments can selectively connect to the inner side of cell membrane (Geiger, 1987; Jones and Green, 1991). Therefore, in the process of cell membrane self-assembly, the inner side of cell membrane is bonded to the electrode surface, while the outer side is exposed. This method ensures that the extracellular domain of hTRPV1 faces the detection substrate. At the same time, type I collagen, as the component of extracellular matrix, was used to fix the cell membrane on the electrode surface. Type I collagen can maintain cell membrane adhesion and provide a stable microenvironment (Gelse et al., 2003). It was observed that the redox peak current decreased further the impedance increased significantly when the cell membrane and type I collagen adhered to the electrode surface. This is due to the blocking of electron transfer caused by the insulation of cell membrane and type I collagen. The CV and EIS characterization confirmed that each modified material was successfully assembled on the electrode surface, indicating the successful construction of the hTRPV1-cell membrane biosensor. The prepared hTRPV1-cell membrane biosensor maintains the complete structure of hTRPV1 through the fixation of cell membrane, so it can be used for the detection of spicy substances.

3.4. Detection of spicy substances

As shown in Fig. S5, the prepared hTRPV1-cell membrane biosensor has the maximum response current change rate to capsaicin at −0.4 V. Fig. S6 shows that the response current stabilizes at 90s. Therefore, under the voltage of −0.4 V, the amperometric i-t curve method was used to detect the three spicy substances. The steady response current of 90s was taken as the measured value. The real-time i-t curves of the three spicy substances detection under different concentrations are shown in Fig. S7. In the gradient concentration detection of capsaicin, allicin and sanshool, the LOD was reached when the concentrations were 1×10^{-15} mol/L, 1×10^{-14} mol/L and 1×10^{-15} mol/L respectively. Taking into account the drawing in a wide gradient concentration range, the concentrations of capsaicin, allicin and sanshool are redefined as follows:

$$pCa_{(\text{capsaicin})} = 16 + \log(C_{(\text{capsaicin})})$$

$$pCa_{(\text{allicin})} = 15 + \log(C_{(\text{allicin})})$$

$$pCa_{(\text{sanshool})} = 16 + \log(C_{(\text{sanshool})})$$

Among them, pCa refers to the redefined concentration of three spicy substances, and C refers to the initial concentration.

The curve was plotted with pCa as the abscissa and the response current change rate as the ordinate. As shown in Fig. 3A–C, when the capsaicin concentration was 1×10^{-15}–1×10^{-13} mol/L, the allicin concentration was 1×10^{-14}–1×10^{-12} mol/L, and the sanshool

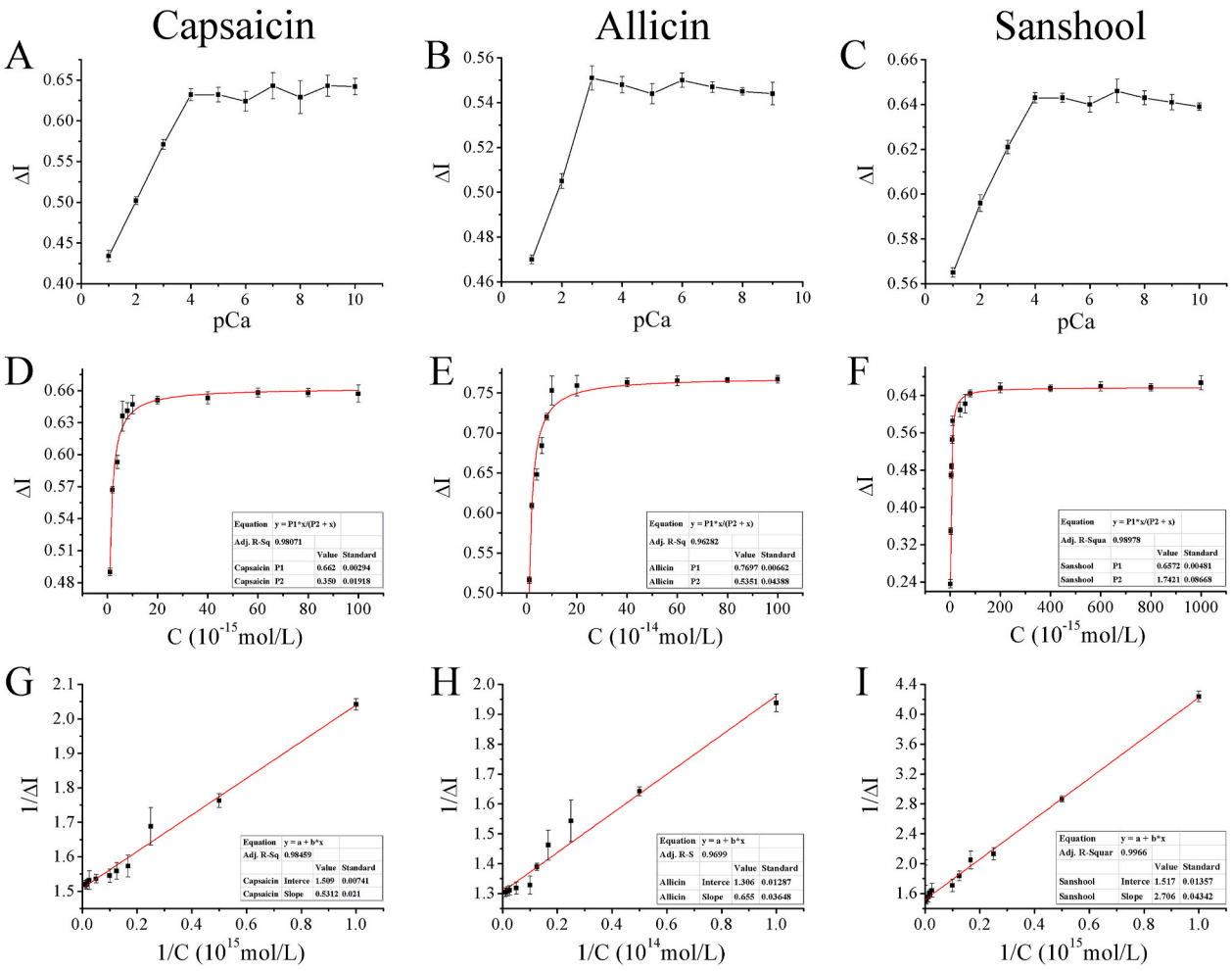

Fig. 3. The detection law of hTRPV1-cell membrane biosensor to three spicy substances. All data show mean ± SD of triplicate measurements. (**A**), (**B**) and (**C**) Detection of the gradient concentration of capsaicin, allicin and sanshool. (**D**), (**E**) and (**F**) A fitting curve of the action law of response current change rate and capsaicin, allicin and sanshool in the linear concentration range respectively. (**G**), (**H**) and (**I**) A fitting curve of the action law between the reciprocal of the response current change rate and the reciprocal of capsaicin, allicin and sanshool concentration in the linear concentration range respectively.

concentration was 1×10^{-15}–1×10^{-12} mol/L, their respective response current change rate had a good linear relationship with pCa. Therefore, the concentration in their linear response range was further subdivided and detected. The kinetic curve was plotted with the concentration of the spicy substance as the abscissa and the response current change rate as the ordinate. By fitting this curve, it was found that there was a good hyperbolic relationship between the change rate of response current and the concentration of spicy substances. The fitting curve was shown in Fig. 3D–F. The fitting equation is:

$$\Delta I_{(\text{capsaicin})} = \frac{0.66252 \times C_{(\text{capsaicin})} \times 10^{-15}}{0.35003 + C_{(\text{capsaicin})} \times 10^{-15}} (R^2 = 0.981)$$

$$\Delta I_{(\text{allicin})} = \frac{0.76972 \times C_{(\text{allicin})} \times 10^{-14}}{0.53518 + C_{(\text{allicin})} \times 10^{-14}} (R^2 = 0.963)$$

$$\Delta I_{(\text{sanshool})} = \frac{0.65723 \times C_{(\text{sanshool})} \times 10^{-15}}{1.74214 + C_{(\text{sanshool})} \times 10^{-15}} (R^2 = 0.990)$$

This indicates that the receptor-ligand binding effect of capsaicin, allicin or sanshool to hTRPV1 is similar to the enzymatic reaction kinetics (Xiao et al., 2019). This is composed of low-concentration first--order reactions, medium-concentration mixed-order reactions and high-concentration zero-order reactions, and has a ligand saturation effect (Warshel, 1984). In other words, when detecting low-concentration spicy substances, the amount of hTRPV1 immobilized on the electrode is greater than that of spicy substances. At this time, the response current change rate is controlled by the concentration of the spicy substance. Therefore, as the concentration of spicy substances increases, the response current change rate gradually increases. However, because the amount of hTRPV1 immobilized on the electrode is limited and constant, when the concentration of spicy substances continues to increase, hTRPV1 is gradually saturated. At this time, the response current change rate is determined by the number of hTRPV1 immobilized on the electrode. Therefore, the response current change rate gradually stabilizes. This is similar to our previous research on the SD rat taste bud tissue sensor (Xiao et al., 2019). Therefore, we can calculate the activation constants of hTRPV1 by capsaicin, allicin, or sanshool by referring to the Michaelis-Menten equation. The activation constant (K_a) is defined as the substrate concentration required to reach half of the maximum output signal of response current change rate. Therefore, we take the reciprocal of the spicy substance concentration as the horizontal axis, and the reciprocal of the response current change rate as the vertical axis to obtain the double reciprocal curve by the Lineweaver-BurkBurk plot method. As shown in Fig. 3G–I. The fitted linear regression equation is as follows:

$$\frac{1}{\Delta I_{(\text{capsaicin})}} = 1.509 + 0.53126 \times \frac{1}{C_{(\text{capsaicin})}} \times 10^{-15} (R^2 = 0.985)$$

$$\frac{1}{\Delta I_{(\text{allicin})}} = 1.30604 + 0.65598 \times \frac{1}{C_{(\text{allicin})}} \times 10^{-14} (R^2 = 0.969)$$

$$\frac{1}{\Delta I_{(\text{sanshool})}} = 1.51757 + 2.70612 \times \frac{1}{C_{(\text{sanshool})}} \times 10^{-15} (R^2 = 0.997)$$

The stimulation of different spicy substances is mainly manifested in the change of K_a value and the maximum response current change rate (V_{max}). Therefore, referring to the calculation method of the Michaelis constant, the calculation formulas of K_a and V_{max} are shown in Eqs. (2) and (3).

$$\text{Slope} = \frac{K_a}{V_{max}} \quad (2)$$

$$\text{Intercept} = \frac{1}{V_{max}} \quad (3)$$

It can be calculated that $K_{a,\ capsaicin} = 3.5206 \times 10^{-16}$ mol/L, $K_{a,\ allicin} = 5.0227 \times 10^{-15}$ mol/L, $K_{a,\ sanshool} = 1.7832 \times 10^{-15}$ mol/L, $V_{max,\ capsaicin} = 0.6627$, $V_{max,\ allicin} = 0.7657$, $V_{max,\ sanshool} = 0.6589$. The K_a value can reflect the affinity of the receptor to the ligand. The smaller the K_a value, the greater the affinity of hTRPV1 with spicy substances. Therefore, the sensitivity order of hTRPV1 to three spicy substances is: capsaicin > sanshool > allicin. And V_{max} reflects the stimulation intensity of spicy substances to hTRPV1. The greater the V_{max} value, the greater the change of the response current of hTRPV1-cell membrane biosensor induced by the spicy substance. Therefore, the stimulation intensity of three spicy substances on hTRPV1 is: allicin > capsaicin > sanshool.

3.5. Repeatability, stability and reproducibility

The ability of the hTRPV1-cell membrane biosensor to continuously detect spicy substances was tested in 3.5×10^{-16} mol/L capsaicin solution. The results are shown in Fig. S8. The relative standard deviation (RSD) value of response current change rate was 2.72%. This shows that the biosensor has good repeatability and can be used for continuous detection.

The prepared hTRPV1-cell membrane biosensor was stored in 0.2 mol/L PBS buffer solution (pH = 7.4), and the 3.5×10^{-16} mol/L capsaicin solution was detected at the same time every day. Fig. 4A shows the stability test results of five prepared biosensors. Obviously, the response current change rate on the seventh day dropped significantly, and the RSD between it and the response current change rate on the sixth day reached 23.61%. This may be due to the long-term immersion in PBS buffer solution, which caused the electrode surface modification material to fall off and the response signal decreased. However, the stability of the hTRPV1-cell membrane biosensor is good within six days.

Finally, we evaluated the reproducibility of the hTRPV1-cell membrane biosensor. Five biosensors were prepared by the same method under the same conditions and used to detect 3.5×10^{-16} mol/L capsaicin (Fig. 4B). The results show that the RSD between the response current change rates of each biosensor is only 0.75%. This indicates that the biosensor can be stably prepared.

3.6. Molecular docking

3.6.1. Analysis of the results of homology-modelling of hTRPV1

The SWISS-MODEL server uses the Qualitative Model Energy ANalysis (QMEAN) scoring function to evaluate the quality of different models. The results showed that the best scoring model (Fig. S9A) was constructed using the TRPV1 structure with a PDBID of 3J5P ($TRPV1_{3J5P}$) as a template (Liao et al., 2013). Due to the lack of ligands in $TRPV1_{3J5P}$ template, the ligand binding center could not be determined. Therefore, we use the "align" function of PyMol to align the

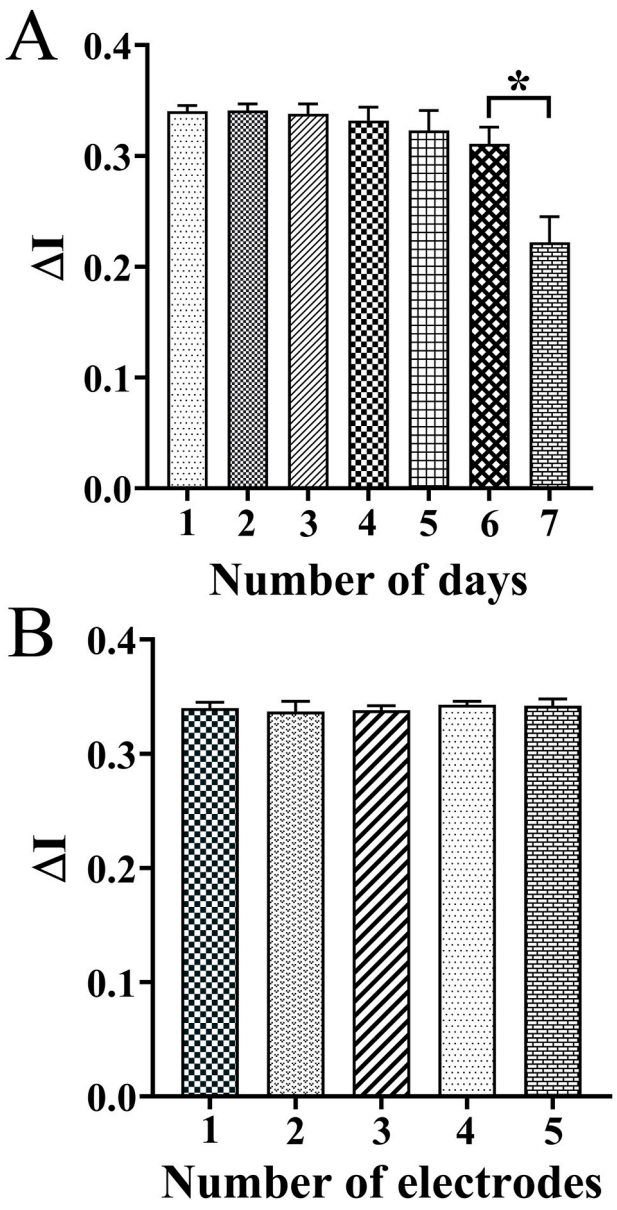

Fig. 4. The stability (A) and reproducibility (B) of hTRPV1-cell membrane biosensor for the detection of spicy substances. 3.5×10^{-16} mol/L capsaicin is used as the test solution.

homology-modelling structure of hTRPV1 ($TRPV1_{3J5P}$ as a template) to the TRPV1 structure with a PDBID of 5IRX ($TRPV1_{5IRX}$) (Gao et al., 2016). This is because the amino acid sequence of $TRPV1_{5IRX}$ and hTRPV1 has the highest homology. In addition, hTRPV1 is a homotetrameric protein composed of four monomers. Therefore, we extracted A Chains from hTRPV1 as receptor ($hTRPV1_A$) for molecular docking (Fig. S9B). Because resiniferatoxin is a super analog of capsaicin, 6EU in $TRPV1_{5IRX}$ was selected as the reference ligand to determine the active pocket. Finally, we obtained the 3D structure of $hTRPV1_A$-6EU.

3.6.2. Feasibility verification of molecular docking

As shown in Fig. S10, the re-docked conformation almost overlaps with the original conformation of 6EU. This indicates that the docking method has good reliability and can be used to study the binding mode of spicy substances and $hTRPV1_A$.

3.6.3. Analysis of molecular docking results

Affinity is the evaluation criterion for the degree of binding between

the target receptor and the small molecule ligand. The higher the affinity value, the stronger the ligand-receptor binding capacity and the more stable the complex formed. The docking results showed that the affinity values of the optimal conformations of the three spicy substances were allicin = −15.0624 kJ/mol, capsaicin = −27.196 kJ/mol and sanshool = −23.012 kJ/mol. Among them, the negative sign represents spontaneous reaction. On the one hand, this proves that the three spicy substances can spontaneously bind to the active pocket of $hTRPV1_A$ without absorbing energy from the outside. On the other hand, the affinity value also indicates that the stability order of the complex formed by the combination of the three spicy substances and $hTRPV1_A$ is: capsaicin > sanshool > allicin. This is completely consistent with the activation constant (K_a value) of the three spicy substances on hTRPV1 measured by the prepared hTRPV1-cell membrane biosensor. This indicates that the prepared biosensor can be used to accurately study the response of hTRPV1 to different spicy substances.

Subsequently, we observed the interactions within the complex at the amino acid level. First, Fig. S11 shows the optimal binding conformations of the three spicy substances in the active pocket of $hTRPV1_A$. The results showed that the three spicy substances were successfully docked into the active pocket of $hTRPV1_A$. Secondly, as shown in Fig. 5, the polar heads of the three spicy substances are inside the active pocket of $hTRPV1_A$ and form hydrogen bonds with amino acid residues. At the same time, the hydrophobic tail of the spicy substance interacts with the non-polar residues outside the active pocket with van der Waals forces. Molecular docking analysis showed that spatial complementarity, hydrophobicity, hydrogen bonding and π-π interactions together promote the combination of spicy substances and $hTRPV1_A$. Finally, we analyzed the specific role of amino acid residues in the process of spicy substances binding to $hTRPV1_A$ through the 2D diagram. As shown in Fig. 6A, the hydrogen bond and Pi-anion interaction of Glu570, Pi-alkyl interaction of Leu553 and Ala566, and carbon-hydrogen bond of Asn551 play a major role in the binding of capsaicin with $hTRPV1_A$. It can be observed from Fig. 6B that the attractive charge of Glu570 and the hydrogen bond of Thr550 and Tyr554 are the keys to the binding of allicin to $hTRPV1_A$. Sanshool shows different characteristics. As shown in Fig. 6C, in addition to the hydrogen bond formed between Glu570 and amino hydrogen of amide group of sanshool, van der Waals force is also very important in the binding process of sanshool and $hTRPV1_A$. Obviously this is related to the longer conjugated double bond in the structure of sanshool. The difference of molecular structure leads to the difference of interaction, and finally caused the difference of affinity of capsaicin, allicin and sanshool with $hTRPV1_A$.

4. Discussion

With reference to the calculation method of Michaelis constant, the activation constants of three spicy substances on hTRPV1 were also obtained through the developed biosensor. This is consistent with the affinity value obtained through the molecular docking experiment. This demonstrates that whether it is the macroscopic result of the sensor or the microscopic result of the molecular level, the order of sensitivity of hTRPV1 to the three spicy substances is: capsaicin > sanshool > allicin. This result is also similar to what people actually feel. In addition, we

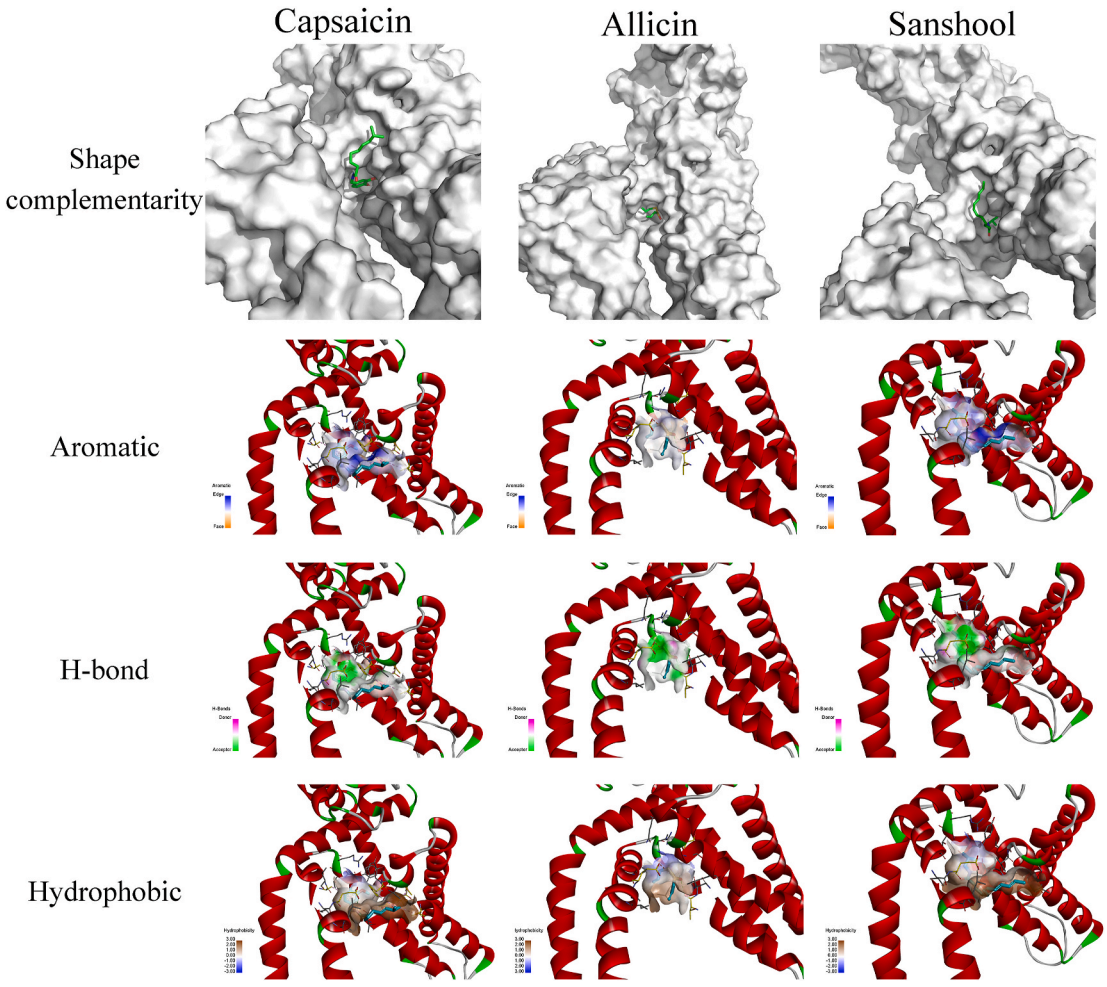

Fig. 5. The interaction of capsaicin, allicin and sanshool with $hTRPV1_A$ active pocket includes shape complementarity, aromatic, hydrogen bond and hydrophobicity.

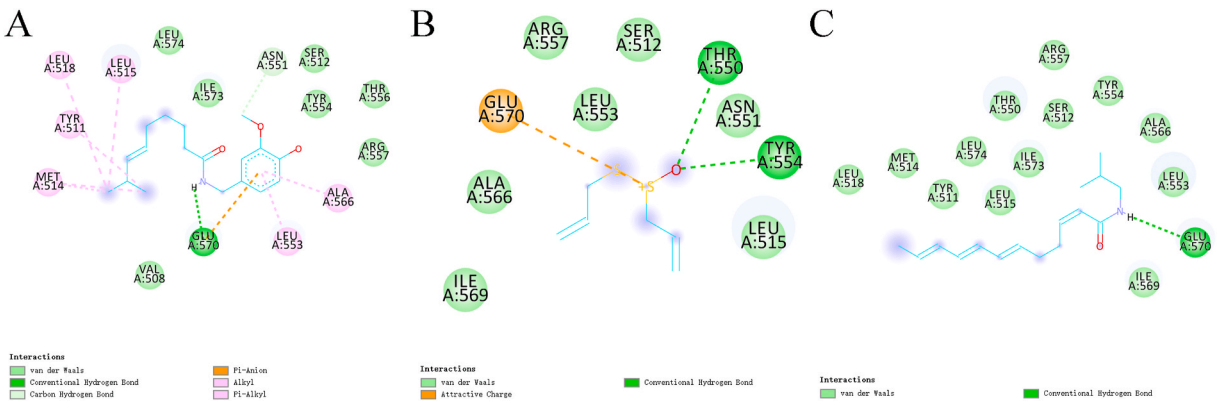

Fig. 6. 2D diagram of the interaction of capsaicin, allicin and sanshool with hTRPV1$_A$. (**A**) Capsaicin. (**B**) Allicin. (**C**) Sanshool.

also analyzed the binding mode of resiniferatoxin and hTRPV1$_A$ (Fig. S12). The results showed that the affinity value of resiniferatoxin to hTRPV1$_A$ was higher than that of capsaicin, reaching −33.8904 kJ/mol, which is consistent with the research results of Maggi et al. (1990). This not only shows that the molecular docking procedure established in this study is accurate, but also that the biosensor results consistent with the molecular docking results are also credible.

After comprehensively analyzing the interaction of 6EU and three spicy substances with hTRPV1$_A$, we found that the amide bond and its similar groups and benzene ring structure play an important role in the binding process of spicy substances and hTRPV1$_A$. Among them, amide bonds and its similar groups mainly participate in the formation of hydrogen bonds, especially the hydrogen bond with Glu570. The benzene ring structure is mainly related to the role of Pi-alkyl interaction. The benzene ring in 6EU and capsaicin makes them show stronger affinity, which just proves the importance of this structure. In the molecular structure of spicy substances, the difference between these two groups is mainly responsible for the diversity in affinity, namely 6EU > capsaicin > sanshool > allicin. This demonstrates a similar conclusion with our previous study based on the SD rat taste bud tissue sensor. Therefore, we believe that the above mentioned structure will be the key to the detection of hTRPV1 activators and the development of analgesics based on inhibitors. In addition, it can be found from Fig. 6B and C that the hydrogen bond of allicin is stronger than that of sanshool, but the affinity of sanshool to hTRPV1 is stronger. This may be due to the aromatic and hydrophobic interaction caused by the long conjugated double bond in the structure of sanshool, which makes the binding of sanshool and hTRPV1 more stable (Fig. 5). It is suggested that the affinity of the spicy substance with hTRPV1 can be increased by appropriately extending the hydrophobic tail of the spicy substance, in addition to ensuring the binding of amide bond and its similar groups and benzene ring structure with the amino acid residues inside the active pocket of hTRPV1. In addition, Glu570 is involved in the binding of all spicy substances with hTRPV1 and plays an irreplaceable role. Therefore, in the study of hTRPV1, Glu570 should be the key focus.

5. Conclusion

In this study, starting from the practical problems of TRPV1 research, a novel hTRPV1-cell membrane biosensor was designed and constructed for the detection of spicy substances. Through the selective adsorption of intermediate filaments and the adhesion of collagen, the cell membrane loaded with hTRPV1 was successfully fixed on the electrode, and the electron transfer efficiency was significantly improved with the help of nano-gold and RGO materials. The results show that the activation constants of capsaicin, allicin and sanshool on hTRPV1 are $K_{a,\ capsaicin} = 3.5206 \times 10^{-16}$ mol/L, $K_{a,\ allicin} = 5.0227 \times 10^{-15}$ mol/L, $K_{a,\ sanshool} = 1.7832 \times 10^{-15}$ mol/L, respectively. Their detection sensitivity order on this biosensor is: capsaicin > sanshool > allicin. This is consistent with the binding mode of the three spicy substances and hTRPV1 simulated by the molecular docking method. The new cell membrane biosensor provides a high sensitivity and low detection limit platform for the direct study of the interaction between hTRPV1 and spicy substance. In addition, the biosensor provides new ideas and methods for the construction of biosensors based on membrane receptors or ion channels. This work is expected to be a model for the development of human-related receptors or protein biosensors.

CRediT authorship contribution statement

Sa Xiao: Conceptualization, Methodology, Formal analysis, Investigation, Writing - original draft, Visualization. **Panpan Song:** Methodology, Formal analysis, Visualization. **Fanjie Bu:** Validation, Investigation. **Guangchang Pang:** Methodology, Writing - review & editing. **Aimin Zhou:** Writing - review & editing. **Yanqing Zhang:** Resources, Supervision. **Junbo Xie:** Writing - review & editing, Project administration, Funding acquisition.

Declaration of competing interest

The authors declare that they have no known competing financial interests or personal relationships that could have appeared to influence the work reported in this paper.

Acknowledgements

This research was supported by the Natural Science Foundation of China (Grant No. 82073989).

Appendix A. Supplementary data

Supplementary data to this article can be found online at https://doi.org/10.1016/j.bios.2020.112779.

References

Bertoni, M., Kiefer, F., Biasini, M., Bordoli, L., Schwede, T., 2017. Sci Rep-UK 7, 10480.
Bienert, S., Waterhouse, A., de Beer, T.A.P., Tauriello, G., Studer, G., Bordoli, L., Schwede, T., 2017. Nucleic Acids Res. 45 (D1), D313–D319.
Boisselier, E., Astruc, D., 2009. Chem. Soc. Rev. 38 (6), 1759–1782.
Cao, E.H., Liao, M.F., Cheng, Y.F., Julius, D., 2013. Nature 504 (7478), 113–118.
Caterina, M.J., Schumacher, M.A., Tominaga, M., Rosen, T.A., Levine, J.D., Julius, D., 1997. Nature 389 (6653), 816–824.
Chang, J.B., Zhou, G.H., Christensen, E.R., Heideman, R., Chen, J.H., 2014. Anal. Bioanal. Chem. 406 (16), 3957–3975.
Chavez-Valdez, A., Shaffer, M.S.P., Boccaccini, A.R., 2013. J. Phys. Chem. B 117 (6), 1502–1515.
Cornell, B.A., BraachMaksvytis, V.L.B., King, L.G., Osman, P.D.J., Raguse, B., Wieczorek, L., Pace, R.J., 1997. Nature 387 (6633), 580–583.

Cui, M., Gosu, V., Basith, S., Hong, S., Choi, S., 2016. Ion channels as therapeutic targets, 104, 81–125. Part B.
Gao, Y., Cao, E.H., Julius, D., Cheng, Y.F., 2016. Nature 534 (7607), 347–351.
Geiger, B., 1987. Nature 329 (6138), 392–393.
Gelse, K., Poschl, E., Aigner, T., 2003. Adv. Drug Deliv. Rev. 55 (12), 1531–1546.
Gerbino, L., Riva, J., Strumia, M., Iglesias, R.A., Baruzzi, A.M., 2008. Sensor. Actuator. B Chem. 131 (2), 455–461.
Gonzalez-Zamora, A., Sierra-Campos, E., Luna-Ortega, J.G., Perez-Morales, R., Ortiz, J.C. R., Garcia-Hernandez, J.L., 2013. Molecules 18 (11), 13471–13486.
Govindarajan, V.S., Narasimhan, S., Dhanaraj, S., 1977. J. Food Sci. Tech. Mys. 14 (1), 28–34.
Guex, N., Peitsch, M.C., Schwede, T., 2009. Electrophoresis 30 (1), S162–S173.
Hammond, G.R.V., Fischer, M.J., Anderson, K.E., Holdich, J., Koteci, A., Balla, T., Irvine, R.F., 2012. Science 337 (6095), 727–730.
Jiang, D.L., Ji, J., An, L., Sun, X.L., Zhang, Y.Z., Zhang, G.Y., Tang, L.L., 2013. Biosens. Bioelectron. 50, 150–156.
Jones, J.C.R., Green, K.J., 1991. Curr. Opin. Cell Biol. 3 (1), 127–132.
Kumar, M.N.V.R., Muzzarelli, R.A.A., Muzzarelli, C., Sashiwa, H., Domb, A.J., 2004. Chem. Rev. 104 (12), 6017–6084.
Lei, Y.M., Xiao, M.M., Li, Y.T., Xu, L., Zhang, H., Zhang, Z.Y., Zhang, G.J., 2017. Biosens. Bioelectron. 91, 1–7.
Liao, M.F., Cao, E.H., Julius, D., Cheng, Y.F., 2013. Nature 504 (7478), 107–112.
Link, S., El-Sayed, M.A., 1999. J. Phys. Chem. B 103 (21), 4212–4217.
Liu, D.L., Wang, W.T., Xing, J.L., Hu, S.J., 2009. Neurosci. Bull. 25 (4), 221–227.
Maggi, C.A., Patacchini, R., Tramontana, M., Amann, R., Giuliani, S., Santicioli, P., 1990. Neuroscience 37 (2), 531–539.
Morris, G.M., Goodsell, D.S., Halliday, R.S., Huey, R., Hart, W.E., Belew, R.K., Olson, A. J., 1998. J. Comput. Chem. 19 (14), 1639–1662.
Morris, G.M., Huey, R., Lindstrom, W., Sanner, M.F., Belew, R.K., Goodsell, D.S., Olson, A.J., 2009. J. Comput. Chem. 30 (16), 2785–2791.
Nilius, B., Szallasi, A., 2014. Pharmacol. Rev. 66 (3), 676–814.
Njoman, M.F., Nugroho, G., Chandra, S.D.P., Permana, Y., Suhadi, S., Mujiono, M., Hermawan, A.D., Sugiono, S., 2017. Br. Food J. 119 (10), 2145–2160.
Oh, S.Y., Cornell, B., Smith, D., Higgins, G., Buffell, C.J., Kok, T.W., 2008. Biosens. Bioelectron. 23 (7), 1161–1165.
Palmieri, V., Papi, M., Conti, C., Ciasca, G., Maulucci, G., De Spirito, M., 2016. Expet Rev. Med. Dev. 13 (11), 1013–1019.
Paup, V.D., Barnett, S.M., Diako, C., Ross, C.F., 2019. J. Food Sci. 84 (9), 2619–2627.
Qiao, L.X., Jiao, L.H., Pang, G.C., Xie, J.B., 2015. Biosens. Bioelectron. 68, 454–461.
Sanner, M.F., 1999. J. Mol. Graph. Model. 17 (1), 57–61.
Schlossareck, C., Ross, C.F., 2019. J. Food Sci. 84 (6), 1563–1569.
Studer, G., Rempfer, C., Waterhouse, A.M., Gumienny, R., Haas, J., Schwede, T., 2020. Bioinformatics 36 (6), 1765–1771.
Tahara, Y., Toko, K., 2013. IEEE Sensor. J. 13 (8), 3001–3011.
Trott, O., Olson, A.J., 2010. J. Comput. Chem. 31 (2), 455–461.
Uto, M., Michaelis, E.K., Hu, I.F., Umezawa, Y., Kuwana, T., 1990. Anal. Sci. 6 (2), 221–225.
Viswanathan, S., Rani, C., Delerue-Matos, C., 2012. Anal. Chim. Acta 726, 79–84.
Warshel, A., 1984. Proc. Acad. Nat. Sci. U. S. A. 81 (2), 444–448.
Watanabe, T., Terada, Y., 2015. J. Nutr. Sci. Vitaminol. 61, S86–S88.
Waterhouse, A., Bertoni, M., Bienert, S., Studer, G., Tauriello, G., Gumienny, R., Heer, F. T., de Beer, T.A.P., Rempfer, C., Bordoli, L., Lepore, R., Schwede, T., 2018. Nucleic Acids Res. 46 (W1), W296–W303.
Weaver, K.M., Luker, R.G., Neale, M.E., 1984. J. Chromatogr. A 301 (1), 288–291.
Wu, S., Yan, K., Li, J.Y., Huynh, R.N., Raub, C.B., Shen, J.N., Shi, X.W., Payne, G.F., 2020. React. Funct. Polym. 148, 104492.
Xiao, S., Zhang, Y.Q., Song, P.P., Xie, J.B., Pang, G.C., 2019. Biosens. Bioelectron. 126, 815–823.
Xia, S.A., Zhu, P., Pi, F.W., Zhang, Y.Z., Li, Y., Wang, J.S., Sun, X.L., 2017. Biosens. Bioelectron. 97, 345–351.
Zhu, Y.W., Murali, S., Cai, W.W., Li, X.S., Suk, J.W., Potts, J.R., Ruoff, R.S., 2010. Adv. Mater. 22 (35), 3906–3924.